

This is the accepted manuscript made available via CHORUS. The article has been published as:

Astrophysical applications of the post-Tolman-Oppenheimer-Volkoff formalism

Kostas Glampedakis, George Pappas, Hector O. Silva, and Emanuele Berti

Phys. Rev. D **94**, 044030 — Published 12 August 2016

DOI: [10.1103/PhysRevD.94.044030](https://doi.org/10.1103/PhysRevD.94.044030)

Astrophysical applications of the post-Tolman-Oppenheimer-Volkoff formalism

Kostas Glampedakis,^{1,2,*} George Pappas,^{3,†} Hector O. Silva,^{3,‡} and Emanuele Berti^{3,4,§}

¹*Departamento de Física, Universidad de Murcia, Murcia, E-30100, Spain*

²*Theoretical Astrophysics, University of Tübingen, Tübingen, D-72076, Germany*

³*Department of Physics and Astronomy, The University of Mississippi, University, MS 38677, USA*

⁴*Departamento de Física, CENTRA, Instituto Superior Técnico, Universidade de Lisboa, Avenida Rovisco Pais 1, 1049 Lisboa, Portugal*

The bulk properties of spherically symmetric stars in general relativity can be obtained by integrating the Tolman-Oppenheimer-Volkoff (TOV) equations. In previous work [1] we developed a “post-TOV” formalism – inspired by parametrized post-Newtonian theory – which allows us to classify in a parametrized, phenomenological form all possible perturbative deviations from the structure of compact stars in general relativity that may be induced by modified gravity at second post-Newtonian order. In this paper we extend the formalism to deal with the stellar exterior, and we compute several potential astrophysical observables within the post-TOV formalism: the surface redshift z_s , the apparent radius R_{app} , the Eddington luminosity at infinity L_E^∞ and the orbital frequencies. We show that, at leading order, all of these quantities depend on just two post-TOV parameters μ_1 and χ , and we discuss the possibility to measure (or set upper bounds on) these parameters.

PACS numbers: 04.40.Dg, 04.50.Kd, 04.80.Cc, 04.25.Nx, 97.60.Jd

I. INTRODUCTION

Compact stars are ideal astrophysical environments to probe the coupling between matter and gravity in a high-density, strong gravity regime not accessible in the laboratory. Cosmological observations and high-energy physics considerations have spurred extensive research on the properties of neutron stars, whether isolated or in binary systems, in modified theories of gravity (see e.g. [2, 3] for reviews). Different extensions of general relativity (GR) affect the bulk properties of the star (such as the mass M and radius R) in similar ways for given assumptions on the equation of state (EOS) of high-density matter. Therefore it is interesting to understand whether these deviations from the predictions of GR can be understood within a simple parametrized formalism. The development of such a generic framework to understand how neutron star properties are affected in modified gravity is even more pressing now that gravitational-wave observations are finally a reality [4], since the observation of neutron star mergers could allow us to probe the dynamical behavior of these objects in extreme environments.

In previous work we developed a post-Tolman-Oppenheimer-Volkoff (henceforth, post-TOV) formalism valid for spherical stars [1]. The basic idea is quite simple. The structure of nonrotating, relativistic stars can be determined by integrating two ordinary differential equations: one of these equations gives the “mass function” and the other equation – a generalization of the hydrostatic equilibrium condition in Newtonian gravity –

determines the pressure profile and the stellar radius, defined as the point where the pressure vanishes. The post-TOV formalism, reviewed in Section II below, adds a relatively small number of parametrized corrections with parameters μ_i ($i = 1, \dots, 5$) and π_i ($i = 1, \dots, 4$) to the mass and pressure equations. These corrections have two properties: (i) they are of second post-Newtonian (PN) order, because first-order deviations are already tightly constrained by observations; and (ii) they are general enough to capture in a phenomenological way all possible deviations from the mass-radius relation in GR. Other parametrizations were explored in [5, 6] by modifying ad hoc the TOV equations.

In this paper we turn to the investigation of astrophysical applications of the formalism. Part of our analysis is inspired by previous work by Psaltis [7], who showed that, under the assumption of spherical symmetry, many properties of neutron stars in metric theories of gravity can be calculated using only conservation laws, Killing symmetries, and the Einstein equivalence principle, without requiring the validity of the GR field equations. Psaltis computed the gravitational redshift of a surface atomic line z_s , the Eddington luminosity at infinity L_E^∞ (thought to be equal to the touchdown luminosity of a radius-expansion burst), and the apparent surface area of a neutron star (which is potentially measurable during the cooling tails of bursts).

We first extend our previous work to study the exterior of neutron stars. Then we compute the surface redshift z_s , the apparent radius R_{app} and the Eddington luminosity at infinity L_E^∞ . In addition, we study geodesic motion in the neutron star spacetime within the post-TOV formalism. We focus on the orbital and epicyclic frequencies, that according to some models – such as the relativistic precession model [8, 9] and the epicyclic resonance model [10] – may be related with the quasi-periodic

* kostas@um.es

† gpappas@olemiss.edu

‡ hosilva@phy.olemiss.edu

§ eberti@olemiss.edu

oscillations (QPOs) observed in the X-ray spectra of accreting neutron stars.

Our main result is that, at leading order, all of these quantities depend on just *two* post-TOV parameters: μ_1 and the combination

$$\chi \equiv \pi_2 - \mu_2 - 2\pi\mu_1. \quad (1)$$

We also express the leading multipoles in a multipolar expansion of the neutron star spacetime in terms of μ_1 and χ , and we discuss the possibility to measure (or set upper bounds on) these parameters with astrophysical observations.

The plan of the paper is as follows. In Section II we present a short review of the post-TOV formalism developed in [1]. In Section III we extend the formalism to deal with the stellar exterior, computing a “post-Schwarzschild” exterior metric. In Section IV we compute the surface redshift z_s and relate it to the stellar compactness M/R . In Section V, following [7], we study the properties of bursting neutron stars in the post-TOV framework. In Section VI we calculate the orbital frequencies. In Section VII we look at the leading-order multipoles of post-TOV stars. Then we present some conclusions and possible directions for future work.

II. OVERVIEW OF THE POST-TOV FORMALISM

Let us begin with a review of the post-TOV formalism introduced in [1]. The core of this formalism consists of the following set of “post-TOV” structure equations for static spherically symmetric stars (we use geometrical units $G = c = 1$):

$$\frac{dp}{dr} = \left(\frac{dp}{dr}\right)_{\text{GR}} - \frac{\rho m}{r^2} (\mathcal{P}_1 + \mathcal{P}_2), \quad (2a)$$

$$\frac{dm}{dr} = \left(\frac{dm}{dr}\right)_{\text{GR}} + 4\pi r^2 \rho (\mathcal{M}_1 + \mathcal{M}_2), \quad (2b)$$

where

$$\mathcal{P}_1 \equiv \delta_1 \frac{m}{r} + 4\pi\delta_2 \frac{r^3 p}{m}, \quad \mathcal{M}_1 \equiv \delta_3 \frac{m}{r} + \delta_4 \Pi, \quad (3a)$$

$$\mathcal{P}_2 \equiv \pi_1 \frac{m^3}{r^5 \rho} + \pi_2 \frac{m^2}{r^2} + \pi_3 r^2 p + \pi_4 \frac{\Pi p}{\rho}, \quad (3b)$$

$$\mathcal{M}_2 \equiv \mu_1 \frac{m^3}{r^5 \rho} + \mu_2 \frac{m^2}{r^2} + \mu_3 r^2 p + \mu_4 \frac{\Pi p}{\rho} + \mu_5 \Pi^3 \frac{r}{m}. \quad (3c)$$

Here r is the circumferential radius, m is the mass function, p is the fluid pressure, ρ is the baryonic rest mass density, ϵ is the total energy density and $\Pi \equiv (\epsilon - \rho)/\rho$

is the internal energy per unit baryonic mass. A “GR” subscript denotes the standard TOV equations in GR, i.e.

$$\left(\frac{dp}{dr}\right)_{\text{GR}} = -\frac{(\epsilon + p)}{r^2} \frac{(m_{\text{T}} + 4\pi r^3 p)}{(1 - 2m_{\text{T}}/r)}, \quad (4a)$$

$$\left(\frac{dm}{dr}\right)_{\text{GR}} = \frac{dm_{\text{T}}}{dr} = 4\pi r^2 \epsilon, \quad (4b)$$

where m_{T} is the GR mass function.

The dimensionless combinations $\mathcal{P}_1, \mathcal{M}_1$ and $\mathcal{P}_2, \mathcal{M}_2$ represent a parametrized departure from the GR stellar structure and are linear combinations of 1PN- and 2PN-order terms, respectively. These terms feature the phenomenological post-TOV parameters δ_i ($i = 1, \dots, 4$), π_i ($i = 1, \dots, 4$) and μ_i ($i = 1, \dots, 5$). In particular, the coefficients δ_i attached to the 1PN terms are simple algebraic combinations of the traditional PPN parameters $\delta_1 \equiv 3(1 + \gamma) - 6\beta + \zeta_2$, $\delta_2 \equiv \gamma - 1 + \zeta_4$, $\delta_3 \equiv -\frac{1}{2}(11 + \gamma - 12\beta + \zeta_2 - 2\zeta_4)$, $\delta_4 \equiv \zeta_3$. As such, they are constrained to be very close to zero by existing Solar System and binary pulsar observations¹: $|\delta_i| \ll 1$. This result translates to negligibly small 1PN terms in Eq. (2): $\mathcal{P}_1 \ll 1$, $\mathcal{M}_1 \ll 1$. On the other hand, π_i and μ_i are presently unconstrained, and consequently $\mathcal{P}_2, \mathcal{M}_2$ should be viewed as describing the dominant (significant) departure from GR. The GR limit of the formalism corresponds to setting all of these parameters to zero, i.e. $\delta_i, \pi_i, \mu_i \rightarrow 0$.

Alternatively, the stellar structure equations (2) can be formally derived – if we neglect the small terms $\mathcal{P}_1, \mathcal{M}_1$ – from a covariantly conserved perfect fluid stress energy tensor [1]:

$$\nabla_\nu T^{\mu\nu} = 0, \quad T^{\mu\nu} = (\epsilon_{\text{eff}} + p)u^\mu u^\nu + pg^{\mu\nu}, \quad (5)$$

where the effective, gravity-modified energy density is

$$\epsilon_{\text{eff}} = \epsilon + \rho\mathcal{M}_2, \quad (6)$$

and the covariant derivative is compatible with the effective post-TOV metric

$$g_{\mu\nu} = \text{diag}[-e^{\nu(r)}, (1 - 2m(r)/r)^{-1}, r^2, r^2 \sin^2 \theta], \quad (7)$$

with

$$\frac{d\nu}{dr} = \frac{2}{r^2} \left[(1 - \mathcal{M}_2) \frac{m + 4\pi r^3 p}{1 - 2m/r} + m\mathcal{P}_2 \right]. \quad (8)$$

This post-TOV metric is valid in the *interior* of the star. In the following section we discuss how an *exterior* post-TOV metric can be constructed within our framework.

¹ Using the latest constraints on the PPN parameters [11] we obtain the following upper limits: $|\delta_1| \lesssim 6 \times 10^{-4}$, $|\delta_2| \lesssim 7 \times 10^{-3}$, $|\delta_3| \lesssim 7 \times 10^{-3}$, $|\delta_4| \lesssim 10^{-8}$.

III. THE EXTERIOR “POST-SCHWARZSCHILD” METRIC

For the applications of the post-TOV formalism considered in this work, we must specify how the g_{tt} and g_{rr} metric elements are calculated in the interior and exterior regions of the fluid distribution. In this section we will construct an exterior spacetime in a “post-Schwarzschild” form.

From the effective post-TOV metric, we have that *inside* the fluid body $g_{tt} = -\exp[\nu(r)]$, where $\nu(r)$ is determined in terms of the fluid variables and post-TOV parameters from Eq. (8). We will assume that *outside* the fluid distribution the *same* effective metric expression holds². Then we get the equations

$$\frac{d\nu}{dr} = \left(\frac{d\nu}{dr}\right)_{\text{GR}} + \frac{2}{r^2} \left[-\mu_2 \frac{m^2}{r^2} \frac{m}{1-2m/r} + \pi_2 \frac{m^3}{r^2} \right], \quad (9)$$

$$\frac{dm}{dr} = 4\pi\mu_1 \frac{m^3}{r^3}, \quad (10)$$

where

$$\left(\frac{d\nu}{dr}\right)_{\text{GR}} \equiv \frac{2}{r^2} \frac{m}{1-2m/r}. \quad (11)$$

These equations originate from the general expressions (8) and (2b) after setting all fluid parameters to zero, i.e. $p = \epsilon = \rho = \Pi = 0$, and keeping the surviving terms in \mathcal{M}_2 and \mathcal{P}_2 . It is not difficult to see that, in the nomenclature of [1], the only 2PN post-TOV terms that can appear in the exterior equations are those of “family F1” and “family F2”. The F1 term (coefficient π_1) should not appear in the \mathcal{P}_2 correction of the *interior* $d\nu/dr$ equation because it is divergent at the surface. This implies that the F1 term should not appear in the dp/dr equation either.

As it stands, Eq. (9) contains higher than 2PN order terms. It should therefore be PN-expanded with respect to the post-TOV terms:

$$\frac{d\nu}{dr} = \left(\frac{d\nu}{dr}\right)_{\text{GR}} + 2(\pi_2 - \mu_2) \frac{m^3}{r^4}. \quad (12)$$

Thus (12) and (10) are our “final” post-TOV equations for the stellar exterior.

The mass equation is decoupled and can be directly integrated. The result is

$$m(r) = \frac{r}{\sqrt{4\pi\mu_1 + Kr^2}}, \quad (13)$$

² This assumption is based on simplicity. While we keep an agnostic view on the validity of Birkhoff’s theorem within our formalism (and in modified gravity theories in general), the interior post-TOV metric is arguably the best guide towards the construction of the exterior metric.

where K is an integration constant. The fact that $dm/dr \neq 0$ outside the star implies the presence of an “atmosphere” due to the non-GR degree of freedom. This is reminiscent of the exterior structure of neutron stars in scalar-tensor theories [12]. The constant K is fixed by setting $m(r \rightarrow \infty)$ equal to the system’s ADM mass M_∞ . Then,

$$m(r) = M_\infty \left(1 + 4\pi\mu_1 \frac{M_\infty^2}{r^2} \right)^{-1/2}. \quad (14)$$

Thus the ADM mass is related to the Schwarzschild mass $M \equiv m(R)$ by

$$M = M_\infty \left(1 + 4\pi\mu_1 \frac{M_\infty^2}{R^2} \right)^{-1/2}. \quad (15)$$

As expected, in the GR limit the two masses coincide

$$m(r > R) = M_\infty = M. \quad (16)$$

Assuming a post-TOV correction $\mathcal{F} \equiv 4\pi|\mu_1|(M_\infty/R)^2 \ll 1$ we can re-expand our result (15),

$$M = M_\infty \left(1 - 2\pi\mu_1 \frac{M_\infty^2}{R^2} \right). \quad (17)$$

The inverse relation $M_\infty = M_\infty(M)$ reads³

$$M_\infty = M \left(1 + 2\pi\mu_1 \frac{M^2}{R^2} \right). \quad (18)$$

The three mass relations (15), (17) and (18) are equivalent in the $\mathcal{F} \ll 1$ limit. Equations (15) and (14) are “exact” post-TOV results and do not require \mathcal{F} or μ_1 to be much smaller than unity, although Eq. (15) does place a lower limit on μ_1 because the argument of the square root must be nonnegative. Unfortunately, the use of (14) in the calculation of the metric components leads to very cumbersome expressions.

To make progress (while also keeping up with the post-TOV spirit), we hereafter use the $\mathcal{F} \ll 1$ approximations (17)-(18). This step, however, introduces a certain degree of error. This is quantified in Fig. 1 (left panel), where we show the relative percent error in calculating M_∞ using the post-TOV expanded Eqs. (17) and (18) rather than Eq. (15). Using EOS Sly4 [13], we considered values of μ_1 for which Eqs. (15) and (17) admit a positive solution for M_∞ . As test beds, we consider neutron stars with central energy densities which result in a canonical $1.4 M_\odot$ and the maximum allowed mass in

³ At first glance, obtaining $M_\infty(M)$ entails solving a cubic equation. However, the procedure is greatly simplified if we recall that the post-TOV formalism must reduce to GR for $\{\mu_i, \pi_i\} \rightarrow 0$. Having that in mind we can treat μ_1 as a small parameter and solve (17) perturbatively. The only regular solution in the $\mu_1 \rightarrow 0$ limit is Eq. (18).

GR, i.e. $2.05 M_\odot$. As evident from Fig. 1, the error can become significant as we increase the value of $|\mu_1|$. By demanding that the errors remain within 5% we can narrow down the admissible values of μ_1 to $[-1.0, 0.1]$. We observe that while M_∞ can deviate greatly from the GR value (e.g. M_∞ reduces by $\approx 21\%$ when $\mu_1 = -1.0$ with respect to a $1.4 M_\odot$ neutron star), \mathcal{F} remains below unity (see right panel of Fig. 1). This is because large negative values of the parameter μ_1 make the star less compact (i.e. Newtonian), as evidenced in Fig. 1 of [1].

We emphasize that the larger errors for some values of μ_1 are not an issue with the post-TOV formalism itself, but serve to constrain the values of μ_1 for which the perturbative expansion is valid. From a practical point of view, excluding large values of $|\mu_1|$ is a sensible strategy, since the resulting stellar parameters are so different with respect to their GR values that these cannot be considered as meaningful post-TOV corrections. Hereafter, whenever we refer to M_∞ we mean the mass calculated using Eq. (18) with $\mu_1 \in [-1.0, 0.1]$.

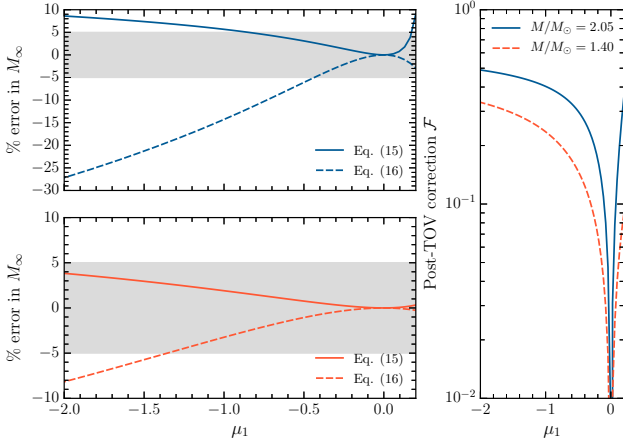


FIG. 1. *Errors in M_∞ .* We show the percent error [% error $\equiv 100 \times (x_{\text{value}} - x_{\text{ref}})/x_{\text{ref}}$] in calculating M_∞ using Eqs. (17) and (18) with respect to (15) for various values of μ_1 using EOS SLy4. The range of μ_1 is chosen such that using any of Eqs. (15), (17) or (18) one can obtain a real root corresponding to M_∞ . The post-TOV models are constructed using a fixed central value of the energy density, which results in either a canonical ($1.4 M_\odot$) or a maximum-mass ($2.05 M_\odot$) neutron star in GR. *Top panel:* errors for a maximum-mass GR star. *Bottom panel:* errors for a canonical-mass GR star. *Right panel:* the absolute value of the post-TOV correction $\mathcal{F} = 4\pi\mu_1(M_\infty/R)^2$ as a function of μ_1 . The condition $\mathcal{F} \ll 1$ bounds the range of acceptable values of μ_1 for which the expansions leading to Eqs. (17) and (18) are valid. Errors are below 5 % when $\mu_1 \in [-1.0, 0.1]$.

Within this approximation we are free to use the Taylor-expanded form of (14), i.e.

$$m(r) = M_\infty \left(1 - 2\pi\mu_1 M_\infty^2 / r^2\right). \quad (19)$$

This expression leads to the exterior g_{rr} metric

$$g_{rr}(r) = \left(1 - \frac{2M_\infty}{r}\right)^{-1} - 4\pi\mu_1 \frac{M_\infty^3}{r^3} + \mathcal{O}\left(\frac{\mu_1 M_\infty^4}{r^4}\right). \quad (20)$$

This expression allows us to identify M_∞ as the space-time's gravitating mass (see also the result for g_{tt} below).

The next step is to use our result for $m(r)$ in (12) and integrate to obtain $\nu(r)$. After expanding to 2PN post-TOV order we obtain:

$$\frac{d\nu}{dr} = \frac{2M_\infty}{r^2} \left(1 - \frac{2M_\infty}{r}\right)^{-1} + 2\chi \frac{M_\infty^3}{r^4}. \quad (21)$$

where the parameter χ , defined in Eq. (1), quantifies the departure from the Schwarzschild metric. Integrating,

$$\nu(r) = \log\left(1 - \frac{2M_\infty}{r}\right) - \frac{2\chi}{3} \frac{M_\infty^3}{r^3}, \quad (22)$$

where the integration constant has been eliminated by requiring asymptotic flatness. The resulting exterior g_{tt} metric component is

$$g_{tt}(r) = -\left(1 - \frac{2M_\infty}{r}\right) + \frac{2\chi}{3} \frac{M_\infty^3}{r^3} + \mathcal{O}\left(\frac{\chi M_\infty^4}{r^4}\right). \quad (23)$$

Eqs. (23) and (20) represent our final results for the 2PN-accurate exterior post-Schwarzschild metric. From this construction it follows that post-TOV stars for which $\mu_1 = \mu_2 = \mu_3 = 0$ have the Schwarzschild metric as the exterior spacetime. The following sections describe how the exterior metric can be used to compute observables of relevance for neutron star astrophysics.

IV. SURFACE REDSHIFT & STELLAR COMPACTNESS

The surface redshift is among the most basic neutron star observables that could be affected by a change in the gravity theory. The surface redshift is defined in the usual way as

$$z_s \equiv \frac{\lambda_\infty - \lambda_s}{\lambda_s} = \frac{f_s}{f_\infty} - 1, \quad (24)$$

where λ and f are the wavelength and frequency of a photon, respectively. Here and below, the subscripts s and ∞ will denote the value of various quantities at the stellar surface $r = R$ and at spatial infinity. The familiar redshift formula

$$\frac{f_\infty}{f_s} = \left[\frac{g_{tt}(R)}{g_{tt}(\infty)}\right]^{1/2} \quad (25)$$

is valid for any static spacetime, regardless of the form of the field equations. Using the metric (23), we easily obtain (at first post-TOV order)

$$\frac{f_s}{f_\infty} = \left(1 - \frac{2M_\infty}{R}\right)^{-1/2} + \frac{\chi}{3} \frac{M_\infty^3}{R^3}. \quad (26)$$

Given that the frequency shift depends only on the ratio M_∞/R , it is more convenient to work in terms of the stellar compactness

$$C = M_\infty/R. \quad (27)$$

Then from the definition of the surface redshift we obtain

$$z_s = z_{\text{GR}} + \frac{\chi}{3}C^3, \quad (28)$$

where

$$z_{\text{GR}} \equiv (1 - 2C)^{-1/2} - 1, \quad (29)$$

is the standard redshift formula in GR, while the second term represents the post-TOV correction. Observe that z_s can be smaller or larger than z_{GR} depending on the sign of the parameter χ . This is shown in Fig. 2 (left panel), where we plot the percent difference $\delta z_s/z_s \equiv 100 \times (z_s - z_{\text{GR}})/z_{\text{GR}}$ as a function of C for two representative cases ($\chi = \pm 0.1$).

A characteristic property of the redshift is that it is a function of C , and as such it cannot be used to disentangle mass and radius individually. A given *observed* surface redshift z_{obs} can be experimentally interpreted either as $z_{\text{obs}} = z_{\text{GR}}(C)$ or $z_{\text{obs}} = z_s(C, \chi)$, and therefore lead to different estimates for C (for a given χ). Fig. 2 (right panel), where we plot the percent difference $\delta C/C \equiv 100 \times (C - C_{\text{GR}})/C_{\text{GR}}$ as a function of z_s , shows how much the inferred compactness would differ in the two cases where $\chi = \pm 0.1$. A positive (negative) χ leads to a lower (higher) inferred compactness with respect to GR. The figure suggests that the “error” in C becomes significant for redshifts $z_s \gtrsim 1$.

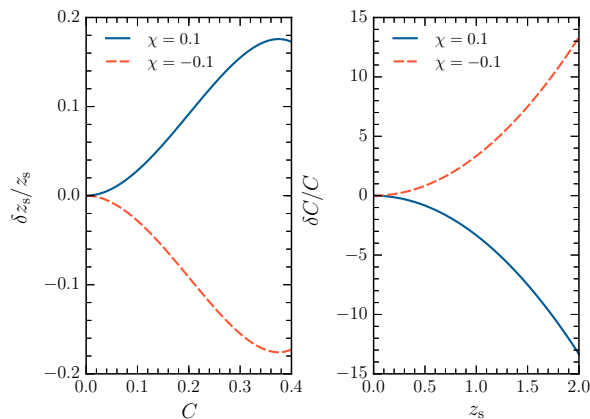


FIG. 2. *Surface redshift and stellar compactness.* Relative percent changes with respect to GR for both z_s and C for different values of χ .

It is a straightforward exercise to invert the redshift formula and obtain a post-TOV expression $C = C(z_s)$. We first write

$$1 + z_s = \frac{1}{\sqrt{-g_{tt}(R)}} \Rightarrow g_{tt}(R) = -\frac{1}{(1 + z_s)^2}. \quad (30)$$

Upon inserting the post-Schwarzschild metric (23) we get a cubic equation for the compactness,

$$-1 + \frac{1}{(1 + z_s)^2} + 2C + \frac{2}{3}\chi C^3 = 0. \quad (31)$$

In solving this equation we take into account that the small parameters are C and $z_s \sim \mathcal{O}(C)$ and that the $\chi \rightarrow 0$ limit should be smooth. We find,

$$C = C_{\text{GR}} \left(1 - \frac{1}{3}\chi z_s^2 \right), \quad (32)$$

where

$$C_{\text{GR}} = \frac{1}{2} [1 - (1 + z_s)^{-2}], \quad (33)$$

is the corresponding solution in GR.

As was the case for the post-TOV redshift formula, the compactness of a post-TOV star can be pushed above (below) the GR value by choosing a negative (positive) parameter χ .

The two main results of this section, Eqs. (28) and (32), are also interesting from a different perspective, namely, their dependence on the single post-TOV parameter χ . This dependence entails a degeneracy with respect to the coefficient triad $\{\mu_1, \mu_2, \pi_2\}$ when (for example) a neutron star redshift observation is used as a gravity theory discriminator. The redshift/compactness χ -degeneracy is another reminder of the intrinsic difficulty in distinguishing non-GR theories of gravity from neutron star physics (see e.g. discussion around Fig. 1 in [1]).

V. BURSTING NEUTRON STARS

A potential testbed for measuring deviations from GR with a parametrized scheme like our post-TOV formalism is provided by accreting neutron stars exhibiting the so-called type I bursts. These are X-ray flashes powered by the nuclear detonation of accreted matter on the stellar surface layers [14]. The luminosity associated with these events can reach the Eddington limit and may cause a photospheric radius expansion (see e.g. [15, 16]), thus offering a number of observational “handles” to the system (see below for more details).

A paper by Psaltis [7] proposed type I bursting neutron stars as a means to constrain possible deviations from GR. Psaltis’ analysis, based on a static and spherically symmetric model for describing the spacetime outside a non-rotating neutron star, is general enough to allow a direct adaptation to the post-TOV scheme. For that reason we can omit most of the technical details discussed in [7] and instead focus on the key results derived in that paper.

There is a number of observable quantities associated with type I bursting neutron stars that can be used to set up a test of GR. The first one is the surface redshift z_s ; in Section IV we have derived post-TOV formulae for

z_s and the stellar compactness C , which are used below in the derivation of a constraint equation between the post-Schwarzschild metric and the various observables.

The luminosity (as measured at infinity) of a source located at a (luminosity) distance D is

$$L_\infty = 4\pi D^2 F_\infty, \quad (34)$$

where F_∞ is the (observable) flux. This luminosity can be written in a black-body form with the help of an apparent surface area S_{app} and a color temperature (as measured at infinity) \bar{T}_∞ :

$$4\pi D^2 F_\infty = \sigma_{\text{SB}} S_{\text{app}} \bar{T}_\infty^4, \quad (35)$$

where σ_{SB} is the Stefan-Boltzmann constant. We then define the second observable parameter used in this analysis, i.e. the apparent radius

$$R_{\text{app}} \equiv \left(\frac{S_{\text{app}}}{4\pi} \right)^{1/2} = D \left(\frac{F_\infty}{\sigma_{\text{SB}} \bar{T}_\infty^4} \right)^{1/2}. \quad (36)$$

As evident from its form, R_{app} is independent of the underpinning gravitational theory, at least to the extent that the theory does not appreciably modify the (luminosity) distance to the source.

The surface color temperature is related to the intrinsic effective temperature T_{eff} via the standard color correction factor f_c [17, 18],

$$\bar{T}_s = f_c T_{\text{eff}}. \quad (37)$$

The observed temperature at infinity picks up a redshift factor with respect to its local surface value, that is,

$$\bar{T}_\infty = f_c \sqrt{-g_{tt}(R)} T_{\text{eff}}. \quad (38)$$

The effective temperature is the one related to the source's intrinsic luminosity,

$$L_s = 4\pi R^2 \sigma_{\text{SB}} T_{\text{eff}}^4. \quad (39)$$

As shown in [7],

$$L_\infty = -g_{tt}(R) L_s = 4\pi R^2 \sigma_{\text{SB}} \left(\frac{\bar{T}_\infty}{f_c} \right)^4 [-g_{tt}(R)]^{-1}. \quad (40)$$

Combining this with the preceding formulae leads to,

$$\frac{R_{\text{app}}}{R} = \frac{1 + z_s}{f_c^2}. \quad (41)$$

The third relevant observable is the Eddington luminosity/flux at infinity. This is given by [7],

$$L_E^\infty = 4\pi D^2 F_E^\infty = \frac{4\pi}{\kappa} \frac{R^2}{(1 + z_s)^2} g_{\text{eff}}, \quad (42)$$

where κ is the opacity of the matter interacting with the radiation field⁴ and g_{eff} is an effective surface gravitational acceleration, defined as:

$$g_{\text{eff}} = \frac{1}{2\sqrt{g_{rr}(R)}} \frac{g'_{tt}(R)}{g_{tt}(R)}. \quad (43)$$

This parameter is key to the present analysis as it encodes the departure from the general relativistic Schwarzschild metric.

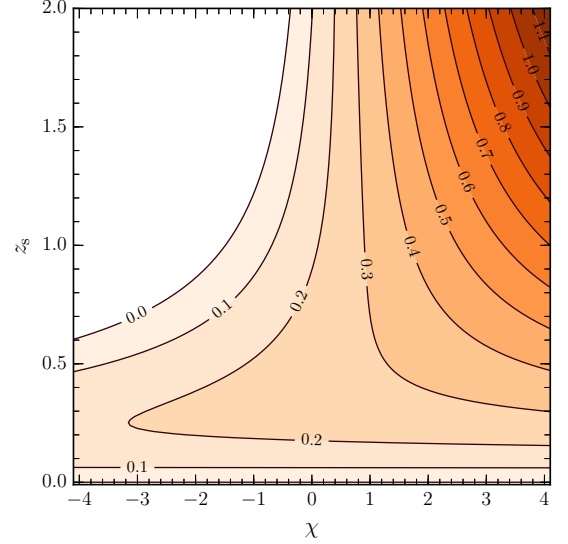


FIG. 3. *Bursting neutron star constraints.* The surfaces are contours of constant $[1 + (2/3)\chi z_s^2] z_s(2 + z_s)/(1 + z_s)^4$ in the (z_s, χ) plane. This quantity is a combination of observables – cf. the right-hand side of Eq. (48) – and therefore it is potentially measurable; a measurement will single out a specific contour in this plot. A further measurement of (say) the redshift z_s corresponds to the intersection between one such contour and a line with $z_s = \text{const.}$, so it can lead to a determination of χ .

Having at our disposal the above three observable combinations, the strategy is to combine them and derive a constraint equation between the observables and the spacetime metric. To this end, we first need to eliminate the not directly observable stellar radius R between (41) and (42) and subsequently solve with respect to g_{eff} . We obtain

$$g_{\text{eff}} = \kappa \sigma_{\text{SB}} \frac{F_E^\infty}{F_\infty} \left(\frac{\bar{T}_\infty}{f_c} \right)^4 (1 + z_s)^4. \quad (44)$$

The remaining task is to express g_{eff} in terms of z_s . Using the post-Schwarzschild metric, Eqs. (20) and (23), in

⁴ Typically, this interaction manifests itself as Thomson scattering in a hydrogen-helium plasma, in which case the opacity is $\kappa \approx 0.2(1 + X) \text{ cm}^2/\text{gr}$ where X is the hydrogen mass fraction [16].

(44) we obtain the post-TOV result

$$g_{\text{eff}} = \frac{C}{R}(1 + z_s)(1 + \chi C^2). \quad (45)$$

Making use of Eq. (32) for the compactness leads to the desired result [cf. Eq. (39) in [7]]:

$$g_{\text{eff}} = \frac{z_s(2 + z_s)}{2R(1 + z_s)} \left(1 + \frac{2}{3}\chi z_s^2 \right), \quad (46)$$

where, as evident, the prefactor represents the GR result. Finally, after eliminating R with the help of (41) and (36), we obtain the “observable” effective gravity:

$$g_{\text{eff}} = \frac{z_s(2 + z_s)}{2Df_c^2} \left(1 + \frac{2}{3}\chi z_s^2 \right) \left(\frac{\sigma_{\text{SB}}\bar{T}_\infty^4}{F_\infty} \right)^{1/2}. \quad (47)$$

This can then be combined with (44) to give

$$\frac{z_s(2 + z_s)}{(1 + z_s)^4} \left(1 + \frac{2}{3}\chi z_s^2 \right) = 2D\kappa \frac{F_E^\infty}{f_c^2} \left(\frac{\sigma_{\text{SB}}\bar{T}_\infty^4}{F_\infty} \right)^{1/2}, \quad (48)$$

and consequently

$$\chi = \frac{3}{2z_s^2} \left[2D\kappa \frac{(1 + z_s)^4}{z_s(2 + z_s)} \frac{F_E^\infty}{f_c^2} \left(\frac{\sigma_{\text{SB}}\bar{T}_\infty^4}{F_\infty} \right)^{1/2} - 1 \right]. \quad (49)$$

This equation is the main result of this section and provides, at least as a proof of principle, a quantitative connection between the post-Schwarzschild correction to the exterior metric [in the form of the χ coefficient defined in Eq. (1)] and observable quantities in a type I bursting neutron star. Ref. [7] arrives at a similar result [their Eq. (49)] which has the same physical meaning, but is not identical to Eq. (48) due to the different assumed form of the exterior metric.

Our results are illustrated in Fig. 3, where we show the left-hand side of Eq. (48) as a contour plot in the (z_s, χ) plane. Each contour represents a specific measurement of this observable quantity. An additional surface redshift measurement can lead, at least in principle, to the determination of the post-TOV parameter χ , as given by Eq. (49).

VI. QUASI-PERIODIC OSCILLATIONS

The post-Schwarzschild metric allows us to compute the geodesic motion of particles in the exterior spacetime of post-TOV neutron stars. Geodesics in neutron star spacetimes play a key role in the theoretical modelling of the QPOs observed in the X-ray spectra of accreting neutron stars. The detailed physical mechanism(s) responsible for the QPO-like time variability in the flux of these systems is still a matter of debate, but some of the most popular models are based on the notion of a radiating hot “blob” of matter moving in nearly circular geodesic orbits. The QPO frequencies are identified

either with the orbital frequencies, or with simple combinations of the orbital frequencies. The most popular models are variants of the relativistic precession [8, 9] and epicyclic resonance [10] models.

In this section we discuss the relevant orbital frequencies within the post-TOV formalism and derive formulae that could easily be used in the aforementioned QPO models. In principle, matching the orbital frequencies to the QPO data would allow one to extract post-TOV parameters such as χ and μ_1 (see [19–21] for a similar exercise in the context of GR and scalar-tensor theory).

For nearly circular orbits in a spherically symmetric spacetime, the only perturbations of interest are the radial ones (i.e., there is periastron precession but no Lense-Thirring nodal precession) and therefore we can associate two frequencies to every circular orbit: the orbital azimuthal frequency of the circular orbit Ω_φ and the radial epicyclic frequency Ω_r .

Geodesics in a static, spherically symmetric spacetime are characterized by the two usual conserved quantities, the energy $E = -g_{tt}\dot{t}$ and the angular momentum $L = g_{\phi\phi}\dot{\phi}$. Here both constants are defined per unit particle mass, and the dots stand for differentiation with respect to proper time. The four-velocity normalization condition $u^a u_a = -1$ yields an effective potential equation for the particle’s radial motion,

$$g_{rr}\dot{r}^2 = -\frac{E^2}{g_{tt}} - \frac{L^2}{g_{\phi\phi}} - 1 \equiv V_{\text{eff}}(r). \quad (50)$$

The conditions for circular orbits are $V_{\text{eff}}(r) = V'_{\text{eff}}(r) = 0$, where the prime denotes differentiation with respect to the radial coordinate. Hereafter r will denote the circular orbit radius. From these conditions we can determine the orbital frequency $\Omega_\varphi \equiv \dot{\phi}/\dot{t}$ measured by an observer at infinity.⁵ The square of the orbital frequency is then given as

$$\Omega_\varphi^2 = -\frac{g'_{tt}}{g'_{\phi\phi}} = \frac{M_\infty}{r^3} \left(1 + \chi \frac{M_\infty^2}{r^2} \right). \quad (51)$$

The Schwarzschild frequency is recovered for $\chi = 0$.

The radial epicyclic frequency can be calculated from the equation for radially perturbed circular orbits, which follows from Eq. (50):

$$\Omega_r^2 = -\frac{g^{rr}}{2\dot{t}^2} V''_{\text{eff}}(r) \approx \frac{M_\infty}{r^3} \left[1 - \frac{6M_\infty}{r} - \frac{\chi M_\infty^2}{r^2} + \mathcal{O}(r^{-3}) \right] \quad (52a)$$

$$= \Omega_\varphi^2 \left[1 - \frac{6M_\infty}{r} - \frac{2\chi M_\infty^2}{r^2} + \mathcal{O}(r^{-3}) \right], \quad (52b)$$

⁵ Apart from its implications for the QPOs, the post-TOV corrected orbital frequency would imply a shift in the corotation radius r_{co} in an accreting system. This radius is defined as $\Omega_* = \Omega_\varphi(r_{\text{co}})$, where Ω_* is the stellar angular frequency, and plays a key role in determining the torque-spin equilibrium in magnetic field-disk coupling models. Using the above definition we find the following result for the post-TOV corotation radius: $r_{\text{co}} = M_\infty(M_\infty\Omega_*)^{-2/3} [1 + (\chi/3)(M_\infty\Omega_*)^{4/3}]$.

where again the frequency is calculated with respect to observers at infinity. From the post-TOV expanded result we can see that the first two terms correspond to the Schwarzschild epicyclic frequency. The additional post-TOV terms in these formulae produce a shift in the frequency and radius of the innermost stable circular orbit (ISCO) with respect to their GR values – the latter quantity is determined by the condition $\Omega_r^2 = 0$, which in GR leads to the well-known result $r_{\text{isco}} = 6M_\infty$. The corresponding post-TOV ISCO is obtained from (52a), up to linear order in χ , as:

$$r_{\text{isco}} \approx 6M_\infty \left(1 + \frac{19}{324}\chi \right). \quad (53)$$

The post-TOV ISCO parameters r_{isco} and $(\Omega_\varphi)_{\text{isco}}$ are plotted in Fig. 4 as functions of the parameter χ . As evident from Eq. (53), a positive (negative) χ implies $r_{\text{isco}} > 6M_\infty$ ($r_{\text{isco}} < 6M_\infty$). If one takes Eq. (52a) at face value for the given post-Schwarzschild metric, for negative enough values of χ there is no ISCO solution, but this occurs well beyond the point where it is safe to use our perturbative formalism. The orbital frequency profile remains rather simple, with $(\Omega_\varphi)_{\text{isco}}$ exceeding the GR value when $r_{\text{isco}} < 6M_\infty$ (and vice versa).

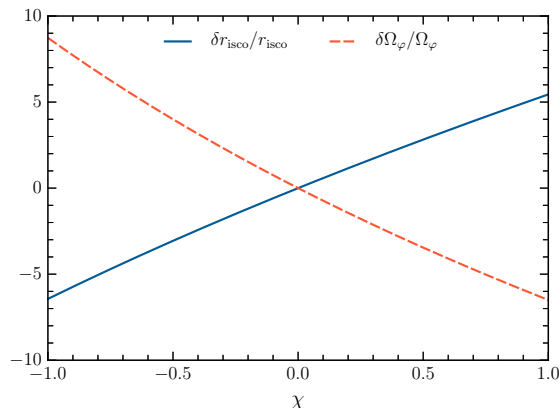


FIG. 4. *ISCO quantities.* ISCO quantities as functions of χ . The solid curve corresponds to the relative difference (in percent) of r_{isco} with respect to GR, while the dashed curve corresponds to the relative difference of the orbital frequency at the ISCO, $(\Omega_\varphi)_{\text{isco}}$.

Besides the frequency pair $\{\Omega_\varphi, \Omega_r\}$, a third prominent quantity in the QPO models is the frequency

$$\Omega_{\text{per}} = \Omega_\varphi - \Omega_r, \quad (54)$$

associated with the orbital periastron precession (for example, in the relativistic precession model [8, 9] this frequency is typically associated with the low-frequency QPO).

Given our earlier results, it is straightforward to derive a series expansion in powers of $1/r$ for Ω_{per} . However,

it is usually more desirable to produce a series expansion with respect to an observable quantity, such as the circular orbital velocity $U_\infty = (M_\infty \Omega_\varphi)^{1/3}$. This can be done by first expanding U_∞ with respect to $1/r$ and then inverting the expansion, thus producing a series in U_∞ . The outcome of this recipe is

$$\frac{\Omega_{\text{per}}}{\Omega_\varphi} = 1 - \frac{\Omega_r}{\Omega_\varphi} = 3U_\infty^2 + \left(\frac{9}{2} + \chi \right) U_\infty^4 + \mathcal{O}(U_\infty^6). \quad (55)$$

A similar “Keplerian” version of this expression can be produced if we opt for using the velocity U_K and mass M_K that an observer would infer from the motion of (say) a binary system under the assumption of exactly Keplerian orbits. These are $U_K = (M_K \Omega_\varphi)^{1/3}$ and $M_K = r^3 \Omega_\varphi^2$, so that $M_K = M_\infty (1 + \chi M_\infty^2 / r^2)$. The resulting series is identical to Eq. (55) when truncated to U_K^4 order. Higher-order terms, however, are different (see the following section).

The above results for the frequencies $\{\Omega_\varphi, \Omega_r, \Omega_{\text{per}}\}$ suggest that a QPO-based test of GR within the post-TOV formalism could in principle allow the extraction of the post-TOV parameter χ . In this sense these frequencies probe the same kind of deviation from GR (and suffer from the same degree of degeneracy) as the observations of bursting neutron stars discussed in Section V.

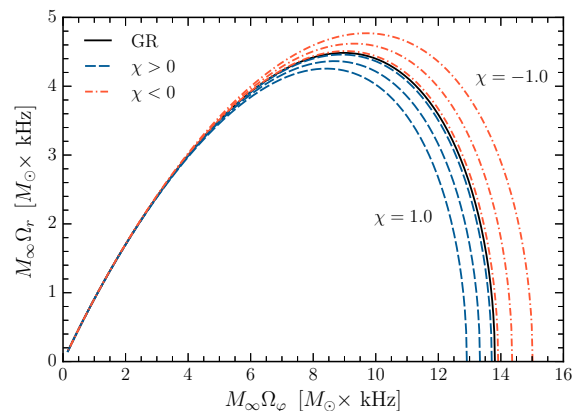


FIG. 5. *Orbital frequencies.* Plots of Ω_r against Ω_φ for different values of $\chi = \pm 0.1, \pm 0.5$ and ± 1 . The black solid curve corresponds to the GR case. The dashed curves correspond to positive values of χ (and $r_{\text{isco}} > 6M_\infty$) while the dashed-dotted curves correspond to negative values of χ (and $r_{\text{isco}} < 6M_\infty$).

We conclude this section by sketching how this procedure works in practice in the context of the relativistic precession model. The twin kHz QPO frequencies $\{\nu_1, \nu_2\}$ seen in the flux of bright low-mass X-ray binaries are identified with the azimuthal and periastron precession orbital frequencies. More specifically, the high-frequency member of the pair is identified with the azimuthal frequency ($\nu_2 = \nu_\varphi = \Omega_\varphi / 2\pi$), while the low-frequency member is identified with the periastron precession ($\nu_1 = \nu_{\text{per}} = \Omega_{\text{per}} / 2\pi$). With this interpretation,

the QPO separation is equal to the radial epicyclic frequency: $\Delta\nu = \nu_2 - \nu_1 = \Omega_r/2\pi$.

We use our previous results [Eqs. (51), (52b), (55)] to plot these orbital frequencies (clearly, $\nu_1/\nu_2 = \Omega_{\text{per}}/\Omega_\varphi$ and $\Delta\nu/\nu_2 = \Omega_r/\Omega_\varphi$) as functions of each other and for varying χ . As it turns out, deviations from GR are best illustrated by plotting $\Omega_r(\Omega_\varphi)$ (or equivalently $\Delta\nu(\nu_2)$). In Fig. 5 we plot the dimensionless combinations $M_\infty\Omega_r$, $M_\infty\Omega_\varphi$ (in units of kHz for the frequencies and solar masses for M_∞). As we can see, the post-TOV models considered here ($-1 < \chi < 1$) are qualitatively similar to the GR result (black solid curve), all cases showing the characteristic hump in Ω_r as Ω_φ increases (so that the orbital radius decreases). This feature is evidently associated with the existence of an ISCO (where $\Omega_r \rightarrow 0$) and is consistent with a similar trend seen in observations [9].

VII. MULTIPOLAR STRUCTURE OF THE SPACETIME

Expansions like Eq. (55) contain information about the multipolar structure of the background spacetime. That expansion can be directly compared against a similar expansion derived by Ryan [19] for an axisymmetric, stationary spacetime in GR with an arbitrary set of mass ($M_0 = M_\infty, M_2, M_4, \dots$) and current (S_1, S_3, S_5, \dots) Geroch-Hansen multipole moments [22–24]:⁶

$$\frac{\Omega_{\text{per}}}{\Omega_\varphi} = 3U^2 - 4\frac{S_1}{M_\infty^2}U^3 + \left(\frac{9}{2} - \frac{3}{2}\frac{M_2}{M_\infty^3}\right)U^4 - 10\frac{S_1}{M_\infty^2}U^5 + \left(\frac{27}{2} - 2\frac{S_1^2}{M_\infty^4} - \frac{21}{2}\frac{M_2}{M_\infty^3}\right)U^6 + \mathcal{O}(U^7). \quad (56)$$

where $U = (M_\infty\Omega_\varphi)^{1/3}$ denotes the orbital velocity.

To understand the PN accuracy of the post-TOV expansion in this context, it is useful to consider the effect of higher PN order terms in the metric. Imagine that the g_{tt} and g_{rr} metric components [see Eqs. (20), (23)] included 3PN corrections of the schematic form,

$$g_{tt}(r) = g_{tt}^{2\text{PN}} + \alpha_{tt}\frac{M_\infty^3}{r^3}, \quad (57)$$

$$g_{rr}(r) = g_{rr}^{2\text{PN}} + \alpha_{rr}\frac{M_\infty^3}{r^3}. \quad (58)$$

We can use the coefficients α_{tt} and α_{rr} as bookkeeping parameters in order to understand how these omitted higher-order contributions affect the results of the previous section. The recalculation of the various expressions reveals that the orbital frequency remains unchanged to

2PN order; the 3PN term of Eq. (57) contributes at the next order, as expected. The same applies to the epicyclic frequency, as we can see for example from the modified Eq. (52b), where the next-order correction is a mixture of $g_{rr}^{2\text{PN}}$ and the 3PN term in g_{tt} :

$$\Omega_r^2 = \Omega_\varphi^2 \left[1 - \frac{6M_\infty}{r} - \frac{2\chi M_\infty^2}{r^2} + \frac{(4\pi\mu_1 - 6\alpha_{tt})M_\infty^3}{r^3} + \mathcal{O}(r^{-4}) \right]. \quad (59)$$

Proceeding in a similar way we find the next-order correction to the Ryan-like expansion (55):

$$\frac{\Omega_{\text{per}}}{\Omega_\varphi} = 3U_\infty^2 + \left(\frac{9}{2} + \chi\right)U_\infty^4 + \left[\frac{27}{2} + 2(\chi - \pi\mu_1) + 3\alpha_{tt}\right]U_\infty^6 + \mathcal{O}(U_\infty^8). \quad (60)$$

We can see that the 3PN term “contaminates” the PN correction that was omitted in Eq. (55). Repeating the same exercise for the Keplerian version of the multipole expansion (i.e. where the orbital velocity U_∞ is replaced by U_K) we find:

$$\frac{\Omega_{\text{per}}}{\Omega_\varphi} = 3U_K^2 + \left(\frac{9}{2} + \chi\right)U_K^4 + \left(\frac{27}{2} - 2\pi\mu_1 + 3\alpha_{tt}\right)U_K^6 + \mathcal{O}(U_K^8). \quad (61)$$

At the PN order considered in the previous section the two expressions were identical but, as we can see, they differ at the next order.

We now have Ryan-type multipole expansions of the post-Schwarzschild spacetime up to 3PN in the circular orbital velocity, which we can compare against Eq. (56) to draw (with some caution) analogies and differences between GR and modified theories of gravity.

For instance, odd powers of U_∞ are missing in Eq. (60) because the nonrotating post-Schwarzschild spacetime has vanishing current multipole moments. Furthermore, we can see that the quadrupole moment M_2 , first appearing in the coefficient of U_∞^4 in Eq. (56), can be associated with χ . The parameter χ is an *effective* quadrupole moment in the sense that

$$M_2^{\text{eff}} = -\frac{2}{3}\chi M_\infty^3. \quad (62)$$

Indeed, this relation implies that a positive (negative) χ could be associated with an oblate (prolate) source of the gravitational field.

The identification (62) holds at $\mathcal{O}(U_\infty^4)$. The next-order term U_∞^6 would, in general, lead to a different effective M_2 . Hence, the comparison between the U_∞^4 and U_∞^6 terms could provide a null test for the GR-predicted quadrupole. However, there is a special case where these two terms could be consistent with the same effective

⁶ A multipolar expansion in scalar-tensor theory can be found in [25]. Specific calculations were also carried out in other theories: for example, the quadrupole moment was computed in Einstein-dilaton-Gauss-Bonnet gravity [26].

quadrupole (62): this occurs when the post-TOV parameters satisfy the condition $5\chi = -2\pi\mu_1 + 3\alpha_{tt}$, in which case the expansion (60) behaves as a “GR mimicker”.

A different kind of “multipole” expansion in powers of $1/r$ can be applied to the metric functions $\nu(r), m(r)$ [see Eqs. (9)–(11)], leading to an alternative calculation of the ADM mass M_∞ of a post-TOV star. We consider the expansions

$$\nu(r) = \sum_{n=0}^{\infty} \frac{\nu_n}{r^n}, \quad m(r) = \sum_{n=0}^{\infty} \frac{m_n}{r^n}, \quad (63)$$

where ν_n and m_n are constant coefficients. In addition, we impose that $\nu_0 = 0$ and $m_0 = M_\infty$. We subsequently substitute these expansions into Eqs. (9)–(10), expand for $r/R \gg 1$, and then solve for the coefficients. The outcome of this exercise in the vacuum exterior spacetime is

$$m(r) = M_\infty - 2\pi\mu_1 \frac{M_\infty^3}{r^2} + \mathcal{O}(r^{-4}), \quad (64)$$

$$\nu(r) = -\frac{2M_\infty}{r} - \frac{2M_\infty^2}{r^2} - \frac{2}{3} \frac{M_\infty^3}{r^3} (4 + \chi) + \mathcal{O}(r^{-4}). \quad (65)$$

As expected, the top equation is consistent with our earlier result, Eq. (19). To get an agreement between Eqs. (22) and (65) we must expand the logarithm appearing in the former equation in powers of M_∞/r , thus recovering Eq. (65).

VIII. CONCLUSIONS

In this paper we have demonstrated the applicability of the post-TOV formalism to a number of facets of neutron star astrophysics. Let us summarize our main results. The exterior post-Schwarzschild metric [Eqs. (20) and (23)] depends only on the ADM mass M_∞ (given by Eq. (18)) and on just two post-TOV parameters μ_1 and χ . These are subsequently used to produce a post-TOV formula for the surface redshift, Eq. (28), which is a function of the stellar compactness and χ . Next, we have shown how a basic post-TOV model for type I bursting neutron stars can be constructed. The key equation here is (49), which gives χ (the only post-TOV parameter appearing in the model) in terms of observable quantities. We also computed geodesic motion in the post-Schwarzschild exterior of post-TOV neutron star models, finding expressions for the orbital, epicyclic and periastron precession frequencies of nearly circular orbits [Eqs. (51), (52b), (55)] and for the ISCO radius [Eq. (53)]. These results can be fed into models for QPOs from accreting neutron stars, such as the relativistic precession model. Finally, on a more theoretical level, we have sketched how the post-TOV parameters enter in the spacetime’s multipolar structure [Eq. (61)].

The meticulous reader may have noticed that, in spite of the exterior metric being a function $g_{tt}(\chi)$ and $g_{rr}(\mu_1)$, all other post-TOV results feature only χ , while μ_1 is either not present or enters at higher order. This is not a coincidence: these quantities either depend solely on g_{tt} (e.g. the redshift) or receive their leading-order contributions from g_{tt} (e.g. the orbital frequencies).

The post-TOV formalism developed in [1] and in this paper can be viewed as a basic “stage-one” version of a more general framework. There are several directions one can follow for taking the formalism to a more sophisticated level, and here we discuss just a couple of possibilities.

An obvious improvement is the addition of stellar rotation. This is necessary because all astrophysical compact stars rotate, some of them quite rapidly, and the influence of rotation is ubiquitous, affecting to some extent all of the effects discussed in this paper. As a first stab at the problem, it would make sense to work in the Hartle-Thorne slow rotation approximation [27, 28], which should be accurate enough for all but the fastest spinning neutron stars [29].

There are equally important possibilities for improvement on the modified gravity sector of the formalism. The present post-TOV theory is oblivious to the existence of dimensionful coupling constants, such as the ones appearing in many modified theories of gravity (e.g. $f(R)$ theories or theories quadratic in the curvature). These coupling parameters should be added to the existing set of fluid parameters, and participate in the algorithmic generation of “families” of post-TOV terms (see [1] for details). The extended set of parameters will most likely lead to a proliferation of post-TOV terms, and result in more complicated stellar structure equations than the ones used so far [i.e. Eqs. (2)]. Among other things, this enhancement may allow one to study in more generality to what extent other theories of gravity are mapped onto the post-TOV formalism. Another limitation of the formalism is that it is intrinsically perturbative with respect to GR solutions. It is important to generalize to theories of gravity that present screening mechanisms; the viability of perturbative expansions in these theories is a topic of active research (see e.g. [30–33]).

We hope that the astrophysical applications outlined in this work will stimulate more research to address these issues.

ACKNOWLEDGMENTS

K.G. is supported by the Ramón y Cajal Programme of the Spanish Ministerio de Ciencia e Innovación and by NewCompStar (a COST-funded Research Networking Programme). H.O.S., G.P. and E.B. are supported by NSF CAREER Grant No. PHY-1055103. E.B. is supported by FCT contract IF/00797/2014/CP1214/CT0012 under the IF2014 Programme. This work was supported by the H2020-MSCA-

RISE-2015 Grant No. StronGrHEP-690904. H.O.S. thanks the Instituto Superior Técnico for hospitality, and

the Department of Physics and Astronomy of the University of Mississippi for financial support.

-
- [1] K. Glampedakis, G. Pappas, H. O. Silva, and E. Berti, *Phys. Rev.* **D92**, 024056 (2015), [arXiv:1504.02455 \[gr-qc\]](#).
 - [2] E. Berti, E. Barausse, V. Cardoso, L. Gualtieri, P. Pani, *et al.*, (2015), [arXiv:1501.07274 \[gr-qc\]](#).
 - [3] N. Yunes and X. Siemens, *Living Rev. Rel.* **16**, 9 (2013), [arXiv:1304.3473 \[gr-qc\]](#).
 - [4] B. P. Abbott *et al.* (Virgo, LIGO Scientific), *Phys. Rev. Lett.* **116**, 061102 (2016), [arXiv:1602.03837 \[gr-qc\]](#).
 - [5] J. Schwab, S. A. Hughes, and S. Rappaport, (2008), [arXiv:0806.0798 \[astro-ph\]](#).
 - [6] H. Velten, A. M. Oliveira, and A. Wojnar (2016) [arXiv:1601.03000 \[astro-ph.CO\]](#).
 - [7] D. Psaltis, *Phys. Rev.* **D77**, 064006 (2008), [arXiv:0704.2426 \[astro-ph\]](#).
 - [8] L. Stella and M. Vietri, *ApJ* **492**, L59 (1998), [astro-ph/9709085](#).
 - [9] L. Stella and M. Vietri, *Phys. Rev. Lett.* **82**, 17 (1999).
 - [10] M. A. Abramowicz and W. Kluzniak, *Astron. Astrophys.* **374**, L19 (2001), [arXiv:astro-ph/0105077 \[astro-ph\]](#).
 - [11] C. M. Will, *Living Rev. Rel.* **17**, 4 (2014), [arXiv:1403.7377 \[gr-qc\]](#).
 - [12] T. Damour and G. Esposito-Farèse, *Phys. Rev. Lett.* **70**, 2220 (1993).
 - [13] F. Douchin and P. Haensel, *Astron. Astrophys.* **380**, 151 (2001), [arXiv:astro-ph/0111092 \[astro-ph\]](#).
 - [14] W. H. G. Lewin, J. van Paradijs, and R. E. Taam, *Space Sci. Rev.* **62**, 223 (1993).
 - [15] E. Kuulkers, P. R. den Hartog, J. J. M. in 't Zand, F. W. M. Verbunt, W. E. Harris, and M. Cocchi, *Astron. Astrophys.* **399**, 663 (2003), [arXiv:astro-ph/0212028 \[astro-ph\]](#).
 - [16] A. W. Steiner, J. M. Lattimer, and E. F. Brown, *Astrophys. J.* **722**, 33 (2010), [arXiv:1005.0811 \[astro-ph.HE\]](#).
 - [17] A. Majczyna, J. Madej, P. C. Joss, and A. Rozanska, *Astron. Astrophys.* **430**, 643 (2005), [arXiv:astro-ph/0412644 \[astro-ph\]](#).
 - [18] V. Suleimanov, J. Poutanen, and K. Werner, *Astron. Astrophys.* **527**, A139 (2011), [arXiv:1009.6147 \[astro-ph.HE\]](#).
 - [19] F. D. Ryan, *Phys. Rev. D* **52**, 5707 (1995).
 - [20] G. Pappas, *MNRAS* **422**, 2581 (2012), [arXiv:1201.6071 \[astro-ph.HE\]](#).
 - [21] G. Pappas and T. P. Sotiriou, *MNRAS* **453**, 2862 (2015), [arXiv:1505.02882 \[gr-qc\]](#).
 - [22] R. P. Geroch, *J. Math. Phys.* **11**, 1955 (1970).
 - [23] R. P. Geroch, *J. Math. Phys.* **11**, 2580 (1970).
 - [24] R. O. Hansen, *J. Math. Phys.* **15**, 46 (1974).
 - [25] G. Pappas and T. P. Sotiriou, *Phys. Rev. D* **91**, 044011 (2015), [arXiv:1412.3494 \[gr-qc\]](#).
 - [26] B. Kleihaus, J. Kunz, and S. Moccia, *Phys. Rev. D* **90**, 061501 (2014), [arXiv:1407.6884 \[gr-qc\]](#).
 - [27] J. B. Hartle, *Astrophys. J.* **150**, 1005 (1967).
 - [28] J. B. Hartle and K. S. Thorne, *Astrophys. J.* **153**, 807 (1968).
 - [29] E. Berti, F. White, A. Maniopolou, and M. Bruni, *Mon. Not. Roy. Astron. Soc.* **358**, 923 (2005), [arXiv:gr-qc/0405146 \[gr-qc\]](#).
 - [30] J. Chagoya, K. Koyama, G. Niz, and G. Tasinato, *JCAP* **1410**, 055 (2014), [arXiv:1407.7744 \[hep-th\]](#).
 - [31] A. Avilez-Lopez, A. Padilla, P. M. Saffin, and C. Skordis, *JCAP* **1506**, 044 (2015), [arXiv:1501.01985 \[gr-qc\]](#).
 - [32] X. Zhang, W. Zhao, H. Huang, and Y. Cai, *Phys. Rev.* **D93**, 124003 (2016), [arXiv:1603.09450 \[gr-qc\]](#).
 - [33] R. McManus, L. Lombriser, and J. Peñarrubia, (2016), [arXiv:1606.03282 \[gr-qc\]](#).